Robotics Reports Volume 3.1, 2025 DOI: 10.1177/28350111251380262 Accepted July 30, 2025



ORIGINAL ARTICLE Open Access

Multivalve Configuration for Soft Robotics: Overcoming the Trade-Off Between Speed and Accuracy in Pneumatic Systems

Taylor R. Young, BEng, Yuen K. Yong, BEng, PhD, and Andrew J. Fleming, BEng, PhD

Abstract

This article describes a new multivalve configuration for achieving both high speed and high resolution in pneumatically driven soft robotic actuators. The proposed method utilizes dual on/off valves with differing orifice sizes in both the charge and discharge paths of the pneumatic circuit. The multiple-valve arrangement provides five states of flow-rate control, which can provide high flow rate for large step changes in pressure, and fine pressure control for precision positioning or force control. Compared with a proportional valve, the proposed method is physically smaller, lower cost, and significantly faster in charging and discharging a soft actuator. The performance of the proposed multivalve system is evaluated using a dual hysteresis control strategy, where the valve combination is dependent on pressure error. The proposed method is experimentally compared with two single-valve configurations, and the results demonstrate a significant improvement in both speed and accuracy. The proposed method is suited to applications that require a fast response between arbitrary set-points and precise control of position or interaction force.

Keywords: multivalve; soft robot; pneumatic system; programmable pressure supply; closed-loop pressure control

Introduction

Fluidic soft robots are traditionally driven by a system of pumps and valves.^{1–3} Their applications include minimally invasive surgery,⁴ rehabilitation,^{5,6} and elderly assistance.⁷ Compared with rigid robots, soft robots provide a desirable combination of high compliance, low mass, and user safety. Soft robots are typically driven by a pneumatic source with on/off valves for pressurization and discharge. Due to the manufacturer-specified minimum mechanical opening time of valves, a trade-off exists between the pressure rise time and the minimum achievable pressure change. The orifice diameter determines the maximum flow rate, while the orifice diameter and minimum on-time determine the

minimum pressure variation. As shown in Figure 1, a large orifice provides a fast response for large pressure changes but is unable to make small pressure variations. Small orifices provide more precise pressure control but have a slow step response for large changes in pressure. This limitation causes the actuator's performance to be constrained by the pneumatic supply rather than the actuator mechanics. As a result, the actuator cannot fully utilize its potential range of motion, force output, or actuation speed, leading to an under-utilized actuator and suboptimal performance. 4,10–12

The main components of compressed air systems are a pump or source, an optional accumulator, and valves for controlling flow direction. ^{13,14} An accumulator can

Precision Mechatronics Lab at the School of Engineering, The University of Newcastle, Callaghan, NSW, Australia.

*Address correspondence to: Taylor R. Young, Precision Mechatronics Lab at the School of Engineering, The University of Newcastle, University Drive, Callaghan, NSW 2308, Australia, Email: taylor.young@newcastle.edu.au

© The Author(s) 2025. Published by Mary Ann Liebert, Inc. This Open Access article is distributed under the terms of the Creative Commons License [CC-BY] (http://creativecommons.org/licenses/by/4.0), which permits unrestricted use, distribution, and reproduction in any medium, provided the original work is properly cited.



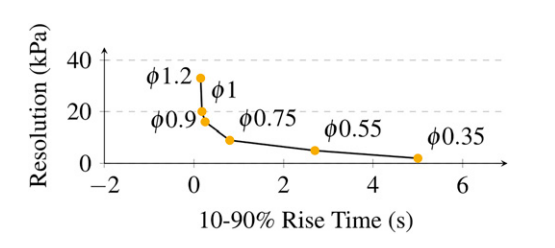


FIG. 1. Trade-off between the speed and resolution of a solenoid valve. The orifice diameter (mm) of the tested valve decreases to the right of the graph. Resolution on the *y*-axis refers to the smallest pressure variation that a pneumatic system can track using the corresponding valve diameter.

also be included to smooth pulsating flow and prevent excessive temporary pressure drop due to sudden demand. ^{15,16} Moreover, the air accumulator allows for reduced energy consumption and fast pressurization of soft actuators. ¹⁷

Various setups with solenoid valves have been described in the soft robotics literature. Systems with 3/2 valves contain a single valve with two states, charging or discharging the actuator. The inlet port is connected to the compressor or the accumulator, the outlet port is connected to the soft actuator, and the exhaust port is open to the atmosphere. These systems have no stable operating point other than maximum inflation and deflation and are not well suited to applications that require arbitrary pressure references.

Most soft robotic systems discharge to ambient pressure, which results in a slow deflation speed as the relative pressure approaches zero. By utilizing a negative pressure source and a second valve, the deflation speed can be improved. However, although the deflation speed is improved, negative pressure is not frequently used due to the need for a vacuum pump and cylinder. Negative pressure also has a tendency to collapse delivery hoses, so the pressure must be chosen conservatively. The methods proposed in this article are equally applicable to systems that use negative pressure or ambient pressure; however, in the remainder of the article, only the more common case of ambient pressure is discussed in detail.

To reduce energy consumption and improve the valve lifetime, more complex 3/3 (3-way, 3-position) or 5/3 (5-way, 3-position) valves can be used.²⁴

However, configurations with higher-order port position combinations are typically more expensive than a system with two 2/2 (2-way, 2-position) valves and provide no further advantage. Systems of two 2/2 valves also provide advantages for the design and manufacturing of custom manifolds, which allow precise selection of the orifice diameter.

Systems utilizing negative pressure have been explored in previous studies. 14,25-27 These systems benefit from the actuator deflation operating point being farther from the source pressure than those relying on atmospheric pressure, leading to reduced actuation times for equivalent step pressure changes. However, despite their performance advantages, they introduce greater complexity to the pneumatic setup. Consequently, they have not been considered in this article, as the proposed method does not depend on the pressure source being distant from the actuator's operating point. Instead, this approach emphasizes the systematic benefits of a dual-valve configuration.

When a system of two 2/2 on/off valves is used, a clear advantage is gained over a system with 3/2 on/off valves due to the additional stable state in which air is neither entering nor exiting the actuator. 9,19,20 The simplest controller is a hysteresis controller with three states. In the first state, valve 1 is used for charging the actuator while valve 2 is blocked. In the second state, both valves are blocked, and no flow is allowed from the accumulator or to the atmosphere. Finally, in the third state, valve 2 is used to discharge the actuator into the atmosphere while valve 1 is blocked. There is a fourth state where both valves are open; however, this state produces no work on the actuator as the air simply travels in and out of the system simultaneously.

Contributions of this work

In this article, two 2/2 valves are proposed to improve the speed and resolution of pneumatically driven soft actuators. The proposed pneumatic system increases the performance of soft actuators without significantly increasing the complexity of the control algorithm or pneumatic system. The two 2/2-valve configuration also offers reduced energy consumption, reduced pressure ripple, and improved lifetime due to a reduced number of switching events compared with a 3/2-valve system.⁹ Hysteresis controllers are implemented to evaluate the speed and accuracy of the proposed methods.

The proposed method is suited to applications that require a fast response between arbitrary set-points and precise control of position or interaction force, such as grippers, exo-suits, and worm-like continuum robots. ^{13,14,17,18,28} In these references, a trade-off was chosen between speed and resolution, which resulted in under-utilization of the soft robotic actuator.

The foremost contributions of this work are:

- A dual arrangement of 2/2 valves is proposed for charging and discharging, as illustrated in Figure 2.
 The dual 2/2 valves are arranged in parallel with orifice diameters selected to optimize both speed and resolution.
- A systematic method is described for choosing the orifice diameters and controller parameters for optimal response.
- The proposed method is experimentally compared with two single-valve configurations. The results demonstrate significant increases in both speed and accuracy.

In the following sections, the dual-valve concept is described in the first section, followed by the experimental system in the second section. A simulation model is presented in the third section, which is used to develop the control algorithm in the fourth section. The characteristics and performance of the proposed method are evaluated in the final section.

Dual-Valve System Concept

Figure 2 illustrates a conventional single-valve system and the proposed multivalve system. The singlevalve system utilizes one on/off valve in both the charge and discharge paths of the pneumatic circuit. This system presents three useful unique flow states. In this article, a comparison system with a singlevalve configuration was chosen because it closely resembles the proposed setup. To ensure a fair comparison between the single-valve and multivalve setups, the same pneumatic valves with the same orifice diameters were used. The dual-valve system utilizes two on/off valves in both the charge and discharge paths of the pneumatic circuit. This configuration presents five useful unique states, which can be chosen to provide a range of flow-rate restrictions. The resolution of a pneumatic system is determined by three main factors:

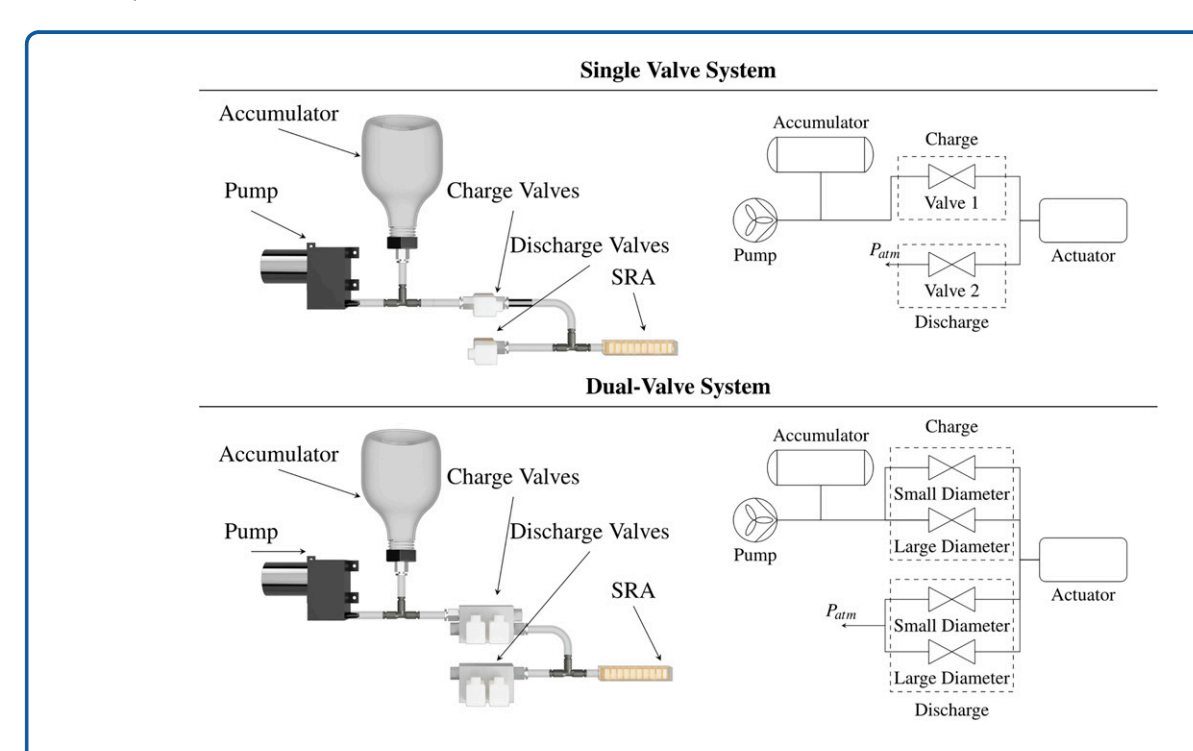


FIG. 2. The single-valve and dual-valve configurations. A pump provides a source of flow into the 1.25 L accumulator. Two pressure sensors are used to measure the accumulator and actuator pressures. A custom manifold with integrated valves is used to create user-defined orifice diameters. The valves are SMC VDW22LA.²⁹

- The difference between the upstream and downstream pressure.
- The pneumatic resistance between the source and actuator, which determines the flow rate.
- The minimum time that a valve can be opened for (minimum on-time).

In a system with a high flow resistance, high pressure resolution can be achieved at the cost of a slow response. Figure 1 compares the rise time and pressure resolution of a pneumatic system with orifice sizes ranging from 0.35 to 1.20 mm and a reservoir pressure of 100 kPa.

The following subsections present an approximate mathematical model to design a desired configuration and determine the optimal flow resistances.

Detailed design

As derived in studies by Xavier et al., ^{14,30} pneumatic systems can be modeled by two fundamental equations, which describe the air pressure dynamics of the pneumatic system. The polytropic gas law models the volume pressurization, which is reasonable for actuators with low deformation due to ballooning, including fast pneumatic network actuators. ^{3,14,30,31}

$$PV^{\gamma} = constant, \tag{1}$$

where *P* is the pressure (in kPa), *V* is the volume, and γ is the polytropic index. In soft robotic applications, ^{17,32–34} the polytropic index is chosen between the isothermal and isentropic processes, $\gamma = 1$ and $\gamma = 1.4$, respectively. In this work, γ is approximated as 1.2.¹⁷

Differentiating both sides of 1,

$$\gamma P V^{\gamma - 1} \frac{dV}{dt} + V^{\gamma} \frac{dP}{dt} = 0 \Rightarrow Q = \frac{V}{\gamma P} \frac{dP}{dt},$$
 (2)

where $Q = -\frac{dV}{dt}$ is the volume flow rate into the actuator (in L/s).

ANSI/(NFPA)T3.21.3 characterizes the volumetric flow rate *Q* (L/s) for charging and discharging through an orifice as,³⁰

$$Q = \frac{114.5C_{v}\sqrt{0.01P_{A}(0.01P_{pump} - 0.01P_{A})}}{\sqrt{T_{R}}},$$
 (3)

where Q (L/s) is the volumetric flow rate through a valve, P_A (kPa) is the actuator pressure, P_{pump} (kPa) is the pump pressure, T_R (K) is the temperature of the air, and C_v is the flow coefficient of the valve.

For an actuator that is charging, by combining Eqs. (2) and (3), the flow rate and pressure of a constant pressure source charging an approximately constant volume load through an orifice is³⁰:

$$\frac{dP_A}{dt} = \frac{\gamma P_A}{V_A} \frac{1.145 \times C_v \sqrt{P_A (P_{pump} - P_A)}}{\sqrt{T_R}},$$
(4)

where the approximately constant volume is V_A (L). This expression shows a nonlinear relationship between the change in pressure dP_A and flow coefficient C_{ν} as well as the upstream and downstream pressures across the charging orifice, P_A and P_{pump} . The flow coefficient C_{ν} is a nonlinear relationship between the upstream, downstream, and orifice diameters and geometry. The worst-case pressure resolution is determined by the minimum on-time of the solenoid valve, which imposes a minimum achievable pressure change dP_A for a given valve flow coefficient or orifice diameter. This minimum change in pressure is a nonlinear function of the upstream and downstream pressures and is greatest when the pressure difference is maximum. To determine the minimum valve on-time, an experiment was conducted by replacing the soft robotic actuator with a small volume. The valve was actuated using short pulse widths ranging from 10 to 30 ms, increasing in 1 ms increments, until a detectable pressure change was observed at the valve's output.

While the valve flow conductance is a function of the pressure difference between the upstream and downstream paths and their absolute values, the following derivation aims to estimate the worst-case pressure resolution within the operating range of the actuator. By rearranging Eq. (4), the required flow coefficient C_v can be approximated as

$$C_{v} = \frac{dP_{A}}{dt} \frac{V_{A}}{\gamma P_{A}} \frac{\sqrt{T_{R}}}{1.145 \sqrt{P_{A}(P_{pump} - P_{A})}}.$$
 (5)

This is discussed in the section "Results." Performance criteria of the system include a 10%–90% rise time \leq 200 ms and an accuracy \leq 2 kPa were first defined. Using Eq. (5), a resolution to 2 kPa and a minimum on-time of 20 ms, the valve conduction coefficient can be calculated C_{ν} = 0.00739. Similarly, by setting the 10%–90% rise time to 200 ms, a resulting value for C_{ν} is 0.02957.

These values were used as starting points to select the orifice diameters of each valve. Second, simulations for a range of single orifices from 0.1 to 2.3 mm were performed to validate the response. This was then experimentally verified to show that the pressure resolution for a 0.35 mm orifice is 1.6 kPa, which agrees with the approximated prediction.

The large orifice was selected using the data, with an orifice of 0.9 mm diameter capable of achieving the 10%–90% rise in approximately 0.192 s.

Experimental System

The experimental system is illustrated in Figure 3 and comprises a diaphragm pump (Keyukang Electronic KYK50BPM³⁵), a 2 L air accumulator, four 2/2 on-off solenoid valves (SMC VDW22LA²⁹), two pressure sensors (Honeywell SSCDANV015PGAA5³⁶), and 6 mm tubing between each of these components. A custom manifold block shown in Figure 4 creates user-defined orifices for each valve. These manifold blocks are 3D printed on a Formlabs Form3 SLA printer in Grey Pro v4 resin. The manifolds were

designed to limit the number of connectors required and minimize leakage. The pump and valves are driven by a PneuSoRD control board. The hysteresis controller is implemented using MATLAB, Simulink, and dSPACE with a MicroLabBox.

The experimental actuator follows the conventional molding procedure for soft fluidic elastomer robots.^{37,38} Molds are designed in Autodesk Fusion 360 and 3D-printed using a Voron Design Voron 2.4. Silicone rubber (DragonSkin 10) is mixed at a 1:1 ratio and degassed. The mixture is poured into the bottom mold, which is then clamped to the top mold. After 5 hours, the actuator is removed, and a strain-limiting layer (fiberglass fabric) is glued to the open side with a layer of DragonSkin.⁹

Modeling and Simulation

A simulation model for the dual-valve system in Figure 3 was developed using Simscape Fluids and

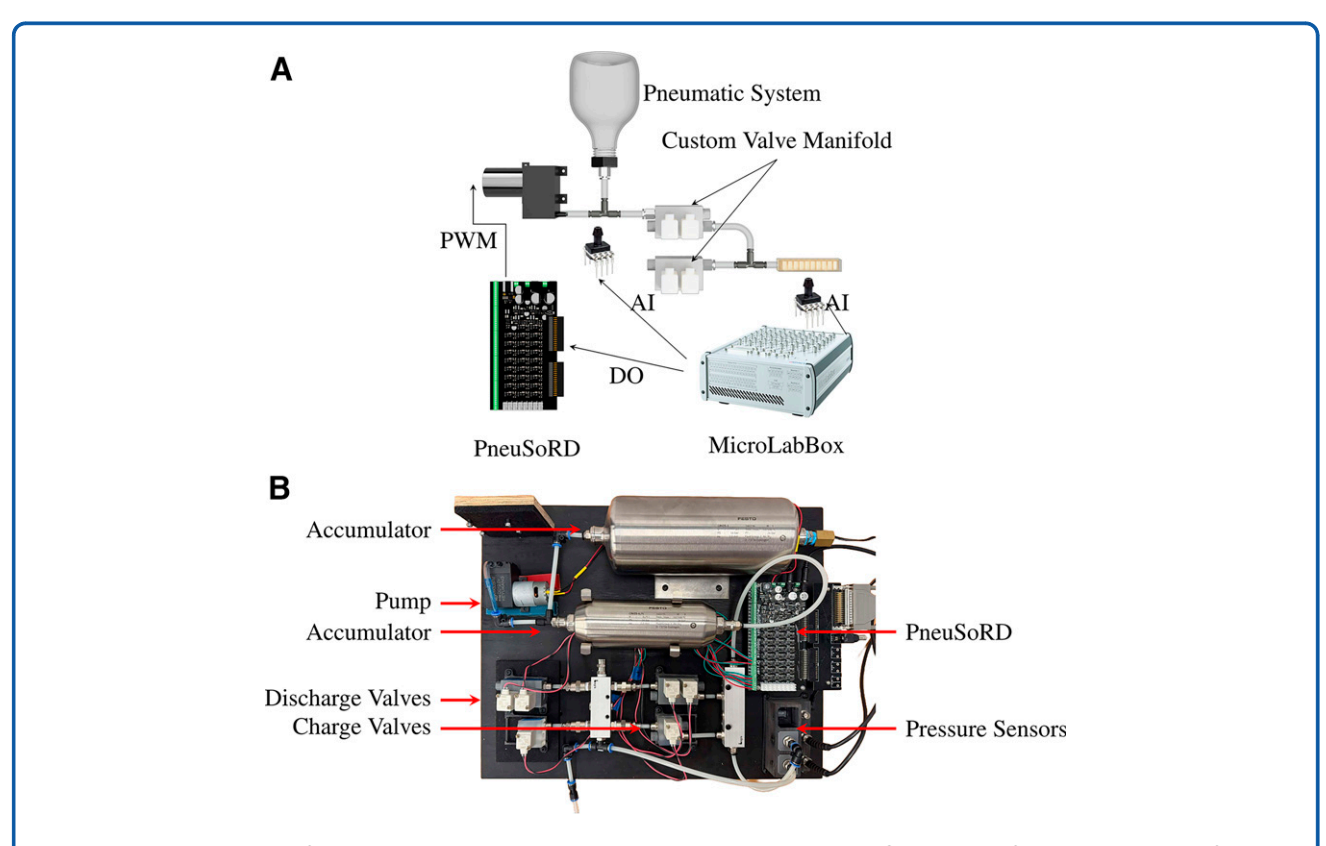


FIG. 3. (A) Render of the experimental system showing the idealized configuration of the custom manifold multivalve setup with dual pneumatic valves. **(B)** Experimental system with dual pneumatic valves. The setup includes a diaphragm pump (KYK50BPM), a 2L accumulator, four 2/2 on–off solenoid valves (VDW22LA), two pressure sensors (SSCDANV015PGAA5, Honeywell), and 6 mm tubing between components.

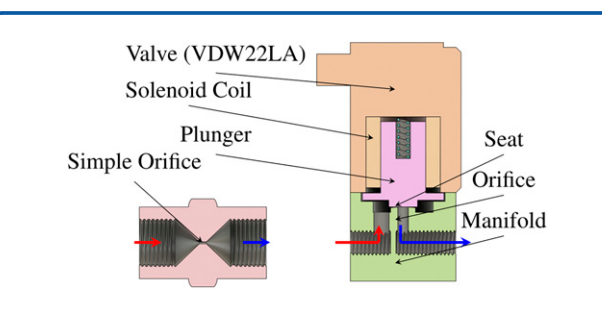


FIG. 4. Cross-section of the two orifice geometries. Left: Airflow through a single conventional orifice. Right: Airflow through a complex valve manifold orifice.

Simulink. As shown in Figure 5, the model includes a flow-rate source, accumulator, pipes, valves, and an actuator modeled by a constant volume. The simulation uses large orifice 2/2 on/off valves in series with smaller orifices to represent the experimental valves described in the section "Experimental System." The ideal controlled volumetric flow source is set to a reference pressure of 100 kPa.

The simulation is used to evaluate the performance of the single-valve and dual-valve setups. Two measurements are taken from these results and used to characterize each orifice size. The first measurement is the rise time (10%–90%), which represents the actuation speed for large changes in pressure. The second measurement is the pressure change recorded 20 ms after the valve is opened, which represents the pressure resolution for a valve with a 20 ms minimum on-time.

Performing these simulations for a range of single orifices from 0.1 to 2.3 mm yields the results in Figure 6. Experimental results are also plotted in Figure 6, which show a similar trend. The difference between the simulated and experimental results is due to the geometric structure and flow coefficient variation between the simulated orifice and experimental orifice. The simulations allow the user to approximate the valve orifice size; however, to select the final valve requirements, experimental data should be used to select the required orifice.

Hysteresis Control

Hysteresis control is used to evaluate the performance of the proposed multivalve system in closed-loop. Hysteresis control allows a direct comparison of performance between a conventional single-valve system and the proposed multivalve system. For a system with single on/off valves, hysteresis control opens one valve at a time, since opening both valves causes direct discharge of pressurized air to the atmosphere. Eliminating this state reduces the number of possible states from 4 to 3. Figure 7A shows the logic output and limits of a symmetric hysteresis controller. When the pressure error exceeds (h_{on}), the charge valve switches on. As the error decreases, the valve remains on until the pressure error is less than (h_{off}) . Similar behavior occurs when the pressure error is negative, thus four control parameters define the behavior. Typically, the hysteresis limits are symmetrically tuned, and the $\pm h_{off}$ is set to 0.

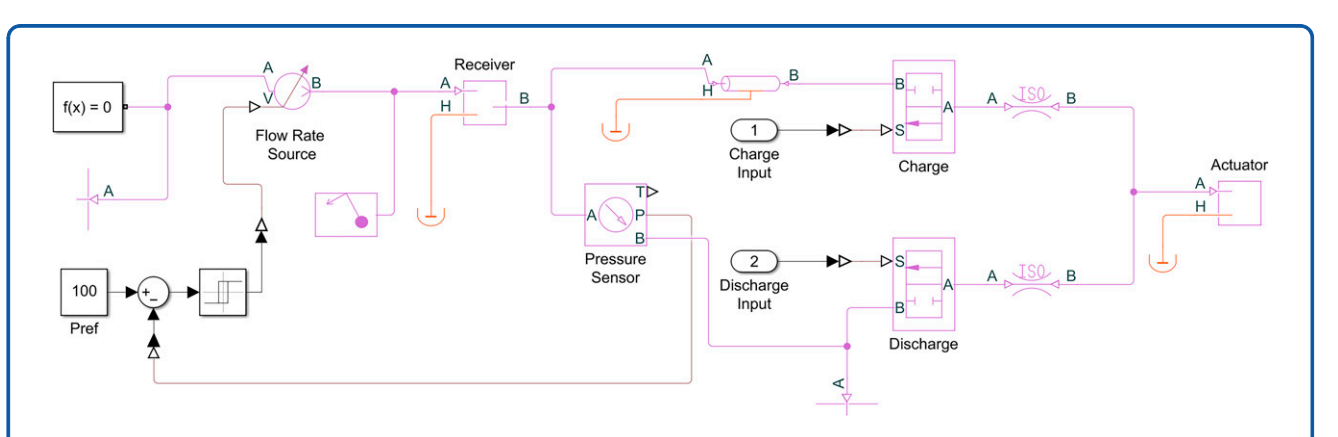


FIG. 5. Simulink model of the pneumatic system. The pneumatic components are shown in magenta and include an air compressor modeled by a controlled volumetric flow source. Transmission pipes represent the pneumatic lines. A constant volume is used to model the actuator.

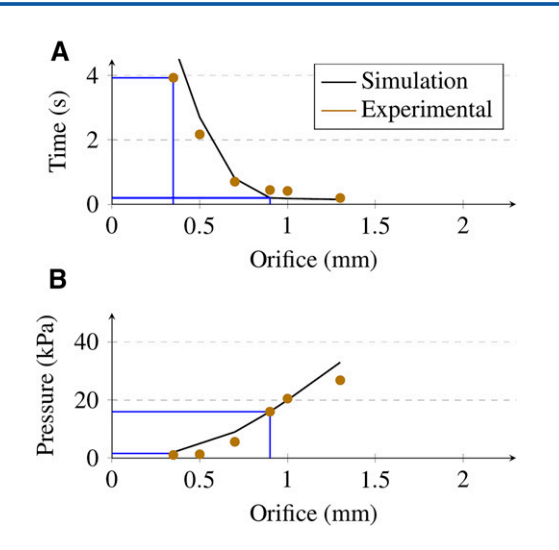


FIG. 6. (A) Step input rise time (10%–90%) versus orifice diameter. **(B)** Pressure resolution for an opening time of 20 ms. The pressure resolution is improved by reducing the orifice diameter. Comparison of simulated and experimental rise time and pressure resolution across a range of orifice diameters. The blue lines indicate the small and large orifices tested. The observed differences between simulation and experiment are attributed to geometric structure and flow coefficient variations between the simulated and experimental orifices.

For a system with dual on/off valves, there are 16 possible states but only five useful states, which are: all valves off (0), slow charge (+1), fast charge (+2), slow discharge (-1), and fast discharge (-2). As shown in Figure 7B, this results in eight controller parameters, or four if they are chosen symmetrically.

Parameter selection

To avoid unnecessary valve activation, the hysteresis limits are chosen slightly greater than the pressure resolution, that is, the minimum achievable pressure change, over all operating conditions. From Eq. (4) the pressure resolution is approximately

$$dP_A = \frac{1.2 \times 1.013}{0.06} \frac{1.145 \times 0.0073 \sqrt{1.013}}{\sqrt{293.15}} \times 0.02,$$

= 2 kPa

where $C_{\nu} = 0.00739$ (0.35 mm orifice). The experimental results in Figure 6B show that the pressure

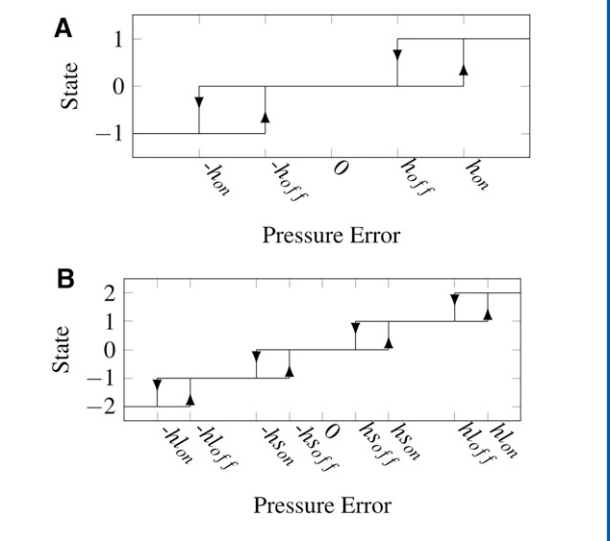


FIG. 7. (A) Single-valve hysteresis controller. **(B)** Dual-valve hysteresis controller. The hysteresis controller output logic versus pressure error for (A) single and (B) dual-valve configurations. States: all valves off (0), slow charge (+1), fast charge (+2), slow discharge (-1), fast discharge (-2).

resolution for a 0.35 mm orifice is 1.6 kPa, which agrees with the approximated prediction. Table 1 compares the experimental pressure resolution for two single valve sizes and a combined dual-valve system.

To eliminate excessive switching due to measurement noise, the hysteresis limits are chosen slightly larger than the pressure resolution. In this article, a safety factor of 1.2 was selected for the on value of the hysteresis controller. That is:

$$hs_{on} = 1.2 \times dP_A$$

$$hs_{off} = 1.2 \times dP_A$$

$$hl_{on} = 1.2 \times dP_A$$

$$hl_{off} = 1.2 \times dP_A$$
(7)

Table 1. Simulated Rise Time and Hysteresis Values for the Selected Orifices

Orifice (mm)	Rise time (s)	Hysteresis (kPa)	
0.35	5	1.60	
0.9	0.19	10.56	
0.35 0.9	0.17	1.6, 10.56 + 1.60	

The data in this table are taken from Figure 6 and used to set the on/off points for the hysteresis controller. The dual orifice is labeled 0.35 $\mid\mid$ 0.9, which means that the two orifice diameters are operated in parallel.

These safety factors were experimentally found to represent a good balance between pressure accuracy and erroneous switching events. Due to the stacked nature of the dual-valve hysteresis controller, the large valve off-time is different for the single and dual-valve controllers. With these safety factors applied, the hysteresis limits are:

• Small valve on: $hs_{on} = 1.92 \text{ kPa}$

• Small valve off: $hs_{off} = 0$ kPa

• Large valve on: $hl_{on} = 14.61 \text{ kPa}$

• Large valve off (single): $hl_{off} = 0$ kPa

• Large valve off (dual): $hl_{off} = 3.21 \text{ kPa}$

Results

The experimental system is designed to achieve the following specifications:

• 10%–90% Rise time ≤200 ms

Accuracy ≤2 kPa

The large orifice was selected using the data in Figure 6A. An orifice with a 0.9 mm diameter is capable of achieving the 10%–90% rise in approximately 0.192 s. This was repeated for the small orifice using the data in Figure 6B. A 0.35 mm orifice has a 20 ms pressure rise of 1.60 kPa; therefore, this was selected as the smaller orifice. In summary, the chosen orifice diameters are:

• Small valve: 0.35 mm

• Large valve: 0.9 mm

• Dual valve: 0.35 mm || 0.9 mm

The notation 0.35 mm || 0.9 mm means that the two orifices are open in parallel. To determine the effectiveness of each controller and valve combination, a series of tests were conducted to compare the speed, accuracy, and ability to track dynamic references. The test conditions are described in the following, and the results are displayed in Figure 8. For each input test, the root mean square (RMS) error is calculated from:

$$RMSE = \sqrt{\frac{\sum (Reference - Actuator \, Pressure)^2}{Number \, of \, Samples}}.$$
 (8)

Speed

The first row of Figure 8 compares the full step of 0–60 kPa for the three configurations under consideration. It can be observed that the single large orifice configuration has a faster response compared with the

single small orifice configuration but a lower accuracy. The dual-valve response exhibits a comparable rise time to the large-orifice system and an accuracy similar to the single small-orifice system.

Accuracy

The second row of Figure 8 compares the ability of each configuration to resolve a 2 kPa step. The system with a single large orifice is unable to track the 2 kPa step, while the single small orifice and dual-valve configurations can track this reference change.

Large step response

The third row of Figure 8 compares the ability of each system to follow large step changes in reference pressure over a range of conditions. The pressure reference is a decreasing-amplitude square wave with a period of 10 s. The small valve system is incapable of settling before the input signal changes, resulting in a significant error. The dual-valve system shows the desirable characteristics of both the single small- and large-orifice systems; that is, the tracking performance is both fast and accurate.

Small step response

The small step response compares the ability of each system to follow a 2 kPa pressure change over a wide range of conditions. The small valve can track the step changes with minimal steady-state error. The system with only large valves is unable to track any of the desired step changes due to the larger required hysteresis band. The response of the dual-valve system is similar to the single small-orifice system.

Dynamic response

The fifth row of Figure 8 has a sinusoidal pressure reference increasing in frequency from 0.1 to 1 Hz over a 100 s period. The single small valve tracks the lower-frequency section of this input reference; however, as the frequency increases, the slew-rate limit eventually results in large tracking errors. On the other hand, the large valve performs best with the higher-frequency input. The lower-frequency signal is quantized by the large hysteresis band, while the dual-valve system combines these two benefits into a single response. A significant improvement over the entire range is shown.

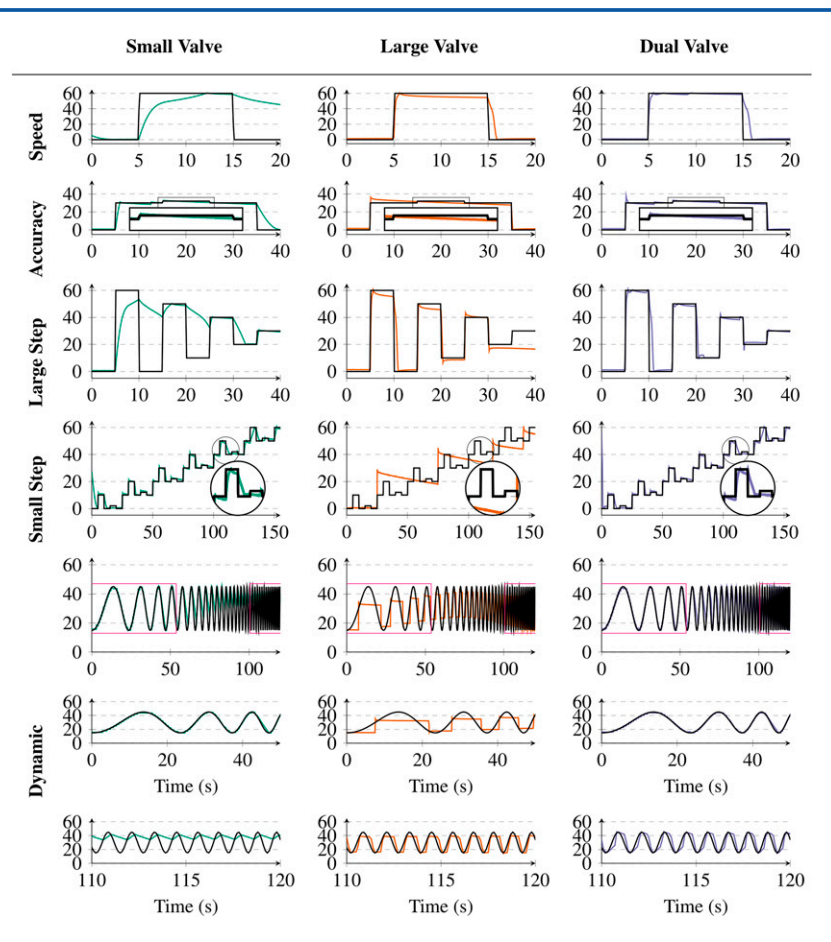


FIG. 8. Experimental comparison of the small-orifice single valve, large-orifice single valve, and dual-valve systems. The *y*-axis of each graph is the actuator pressure in kPa. Each column represents the experimental configuration tested, and each row represents a different test condition, which is discussed in the following: Speed—a full-range step input shows that the rise times of the large-orifice and dual-orifice systems are significantly faster than the small-orifice system, which is expected; Accuracy—a 2 kPa step demonstrates the ability of the small single-valve and dual-valve systems to track the desired 2 kPa pressure change; Large step—a series of decreasing-amplitude steps demonstrates that the dual-valve system simultaneously provides a fast rise time and high pressure accuracy; Small step—a series of 2 and 10 kPa step changes demonstrates that only the small-orifice and dual-orifice systems can track small changes in reference pressure; Dynamic—a sinusoidal wave increasing in frequency from 0.1 to 1 Hz over a 100 s period. The second axis zooms in on the interval from 0 to 50 s. The third axis zooms in on the interval from 60 to 80 s. All of the experiments demonstrate that the dual-valve system can simultaneously achieve the high speed of a large-orifice valve and the high resolution of a small-orifice valve.

Performance comparison

The RMS error for each experiment is summarized in Table 2. The dual-valve system is observed to consistently outperform the single small- and large-orifice systems. Further efforts could be made to include a negative source for improved deflation performance.

Comparison of valve configurations

Table 3 presents a comparison of different pneumatic valve configurations. While 3/2 valves are commonly used due to their affordability and ease of implementation, particularly in fluidic control boards, 2/2 valves offer notable advantages. These include lower energy consumption, reduced pressure fluctuations, and



Table 2. RMS Tracking Error of the Results Plotted in Figure 8

Orifice (mm)	Single 0.35 mm	Single 0.9 mm	Dual valve 0.35 0.9 mm
Speed	27.83	8.69	8.96
Accuracy	5.37	2.35	1.69
Large step	21.60	8.32	7.35
Small step	3.11	8.10	3.61
Dynamic	7.86	6.79	4.82

In each experiment, the dual-valve system matches or achieves a significant improvement in performance over the single-valve systems.

enhanced longevity due to fewer switching events, especially for constant pressure set points. Proportional valves, though more complex in terms of drive and control design, have not demonstrated a significant reduction in tracking error. Consequently, a pneumatic system utilizing two 2/2 on–off valves is recommended for most applications.

Conclusion

This article describes a method for increasing the speed and accuracy of pneumatic soft robotic actuators. A dual-valve arrangement with optimized orifice sizes is proposed for the charge and discharge path. A design procedure is described for the orifice diameters and control parameters. A dual hysteresis controller, which allows independent tuning of the switching conditions for each orifice, was implemented to evaluate the performance of the proposed pneumatic system.

The proposed dual-valve system is experimentally compared with single-valve systems with a large and small orifice. The dual-valve system exhibits the high speed of large-orifice valves and the high resolution of small-orifice valves. Therefore, the proposed method provides a significant performance improvement for

Table 3. Comparison of Pneumatic Systems Relative to the Proposed Configuration^{8,9,14}

Setup	Cost	Lifetime	Volume	Complexity	Accuracy
3/2 on–off valve	0.6	0.1	0.2	0.5	5.0
2/2 on-off valves	0.5	1.1	0.5	0.5	3.0
Dual 2/2 on–off valves	1.0	1.0	1.0	1.0	1.0
2/2 prop. valves	4.3+	1.0	0.7–1.7	2.0	1.0

All valves have similar orifice diameters. Where possible, costs were sourced from the same manufacturer and supplier. Lifetime is assessed based on the number of valve switches required to achieve equivalent performance. Volume is estimated by considering the total setup size, including component connections within the system. Complexity is evaluated based on the electronic and control requirements for operating each configuration. Accuracy reflects the overall control performance across the three test signals.

applications that require both high speed and resolution. This pneumatic system is best suited to tethered applications where large pressure sources and an increase in the number of valves do not negatively impact the function of the robot.

Applications are expected to include soft grippers, catheter devices, and soft robotic limbs, including fingers and hands. Future work will focus on optimizing the selection of valve orifice diameter and improving the control strategy for dynamic trajectories.

Author Disclosure Statement

No competing financial interests exist.

Funding Information

No funding was received for this article.

References

- Polygerinos P, Correll N, Morin SA, et al. Soft robotics: Review of fluiddriven intrinsically soft devices; manufacturing, sensing, control, and applications in human-robot interaction. Adv Eng Mater 2017;19(12): 1700016.
- Gorissen B, Reynaerts D, Konishi S, et al. Elastic inflatable actuators for soft robotic applications. Adv Mater 2017;29(43):1604977; doi: 10.1002/ adma.201604977
- Xavier MS, Fleming AJ, Yong YK. Finite element modeling of soft fluidic actuators: Overview and recent developments. Adv Intell Syst 2021;3(2): 2000187. doi: 10.1002/aisy.202000187
- 4. Runciman M, Darzi A, Mylonas GP. Soft robotics in minimally invasive surgery. Soft Robot 2019;6(4):423–443.
- Polygerinos P, Lyne S, Wang Z, et al. Towards a soft pneumatic glove for hand rehabilitation. In: IEEE/RSJ IEEE Int. Conf. on Intelligent Robots and Systems. IEEE; 2013, pp. 1512–7.
- Wehner M, Quinlivan B, Aubin PM, et al. A lightweight soft exosuit for gait assistance. In: 2013 IEEE International Conference on Robotics and Automation. IEEE; 2013, pp. 3362–9. ISSN: 1050-4729. Available from: https://ieeexplore.ieee.org/document/6631046
- Ansari Y, Manti M, Falotico E, et al. Towards the development of a soft manipulator as an assistive robot for personal care of elderly people. Int J Adv Robotic Syst 2017;14(2):1729881416687132.
- Xavier MS, Fleming AJ, Yong YK. Design and control of pneumatic systems for soft robotics: A simulation approach. IEEE Robot Autom Lett 2021;6(3):5800–5807.
- Young TR, Xavier MS, Yong YK, et al. A control and drive system for pneumatic soft robots: PneuSoRD. In: 2021 IEEE/RSJ International Conference on Intelligent Robots and Systems (IROS). IEEE; 2021, pp. 2822–9.
- 10. Wan Z, Sun Y, Qin Y, et al. Design, analysis, and real-time simulation of a 3D soft robotic snake. Soft Robot 2023;10(2):258–268.
- Jain S, Dontu S, Teoh JEM, et al. A multimodal, reconfigurable workspace soft gripper for advanced grasping tasks. Soft Robot 2023;10(3): 527–544.
- Ambrose JW, Chiang NZR, Cheah DSY, et al. Compact multilayer extension actuators for reconfigurable soft robots. Soft Robot 2023;10(2): 301–313.
- 13. Joshi S, Paik J. Pneumatic supply system parameter optimization for soft actuators. Soft Robot 2021;8(2):152–163.
- Xavier MS, Tawk CD, Zolfagharian A, et al. Soft pneumatic actuators: A review of design, fabrication, modeling, sensing, control and applications. IEEE Access 2022;10:59442–59485.
- Jagadeesha T. Pneumatics: Concepts, Design and Applications. Universities Press; 2015.



- Parr A. Hydraulics and Pneumatics, 3rd ed. Butterworth-Heinemann;
 2011. Available from: https://www.sciencedirect.com/science/article/pii/B978008096674800001X
- Xavier MS, Fleming AJ, Yong YK. Modelling and Simulation of Pneumatic Sources for Soft Robotic Applications. In: 2020 IEEE/ASME International Conference on Advanced Intelligent Mechatronics (AIM). IEEE; 2020, pp. 916–21. ISSN: 2159-6255. Available from: https://ieeexplore.ieee.org/ document/9158802
- Skorina EH, Luo M, Tao W, et al. Adapting to flexibility: Model reference adaptive control of soft bending actuators. IEEE Robot Autom Lett 2017; 2(2):964–970.
- Booth JW, Case JC, White EL, et al. An addressable pneumatic regulator for distributed control of soft robots. In: 2018 IEEE International Conference on Soft Robotics (RoboSoft). IEEE; 2018, pp. 25–30. Available from: https://ieeexplore.ieee.org/document/8404892
- Wang T, Zhang Y, Chen Z, et al. Parameter Identification and Model-Based Nonlinear Robust Control of Fluidic Soft Bending Actuators. IEEE/ASME Trans Mechatron 2019;24(3):1346–1355.
- Skorina EH, Luo M, Ozel S, et al. Feedforward augmented sliding mode motion control of antagonistic soft pneumatic actuators. In: 2015 IEEE International Conference on Robotics and Automation (ICRA). IEEE; 2015. pp. 2544–9. ISSN: 1050-4729. Available from: https://ieeexplore.ieee.org/document/7139540
- Zhang B, Chen J, Ma X, et al. Pneumatic system capable of supplying programmable pressure states for soft robots. Soft Robot 2022;9(5): 1001–1013.
- 23. Xiao X, Huang K, Zhu R, et al. Programmable Pressure Pneumatic System for Soft Robots. In: 2023 IEEE International Conference on Robotics and Biomimetics (ROBIO). IEEE; 2023, pp. 1–6. Available from: https://ieeexplore.ieee.org/document/10354842
- Khan AH, Shao Z, Li S, et al. Which is the best PID variant for pneumatic soft robots? an experimental study. IEEE/CAA J Autom Sinica 2020;7(2): 451–460.
- Tawk C, Alici G. A review of 3D-printable soft pneumatic actuators and sensors: Research challenges and opportunities. Adv Intell Syst 2021; 3(6):2000223. Available from: https://advanced.onlinelibrary.wiley.com/ doi/pdf/10.1002/aisy.202000223
- Kalisky T, Wang Y, Shih B, et al. Differential pressure control of 3D printed soft fluidic actuators. In: 2017 IEEE/RSJ International Conference on Intelligent Robots and Systems (IROS). IEEE; 2017. pp. 6207–13. ISSN: 2153-0866. Available from: https://ieeexplore.ieee.org/document/8206523
- Xavier MS, Tawk CD, Yong YK, et al. 3D-printed omnidirectional soft pneumatic actuators: Design, modeling and characterization. Sensors and Actuators A: Physical 2021;332:113199.
- 28. George Thuruthel T, Ansari Y, Falotico E, et al. Control strategies for soft robotic manipulators: A survey. Soft Robot 2018;5(2):149–163.
- SMC. SMC. Series VDW; 2022. Available from: https://www .smcpneumatics.com/pdfs/VDW.pdf [Last accessed: June 1, 2022].

- Xavier MS, Fleming AJ, Yong YK. Model-based nonlinear feedback controllers for pressure control of soft pneumatic actuators using On/Off valves. Front Robotics Al. 2022;9. Publisher: Frontiers.
- Chen C, Tang W, Hu Y, et al. Fiber-reinforced soft bending actuator control utilizing on/off valves. IEEE Robot Autom Lett 2020;5(4):6732–6739.
- Richer E, Hurmuzlu Y. A high performance pneumatic force actuator system: Part I—nonlinear mathematical model. J Dynamic Syst Measurement Control 2000:122(3):416–425.
- Carneiro JF, de Almeida FG. Reduced-Order Thermodynamic Models for Servo-Pneumatic Actuator Chambers. In: Proceedings of the Institution of Mechanical Engineers, Part I: Journal of Systems and Control Engineering, vol. 220. IMECHE; 2006; pp. 301–14.
- Al-Ibrahim AM. Transient Air Temperature and Pressure Measurements
 During the Charging and Discharging Processes of an Actuating Pneumatic Cylinder. University of Wisconsin–Madison; 1991. Google-Books-ID: 0axKAAAAMAAJ.
- Micro Air Pump 6V/12V/24V 1300mmHg 10L/min 50APM/50BPM Beauty Instrument; 2024. Available from: Available from: https://hsh-flo-store .com/products/micro-air-pump-6v-12v-24v-1300mmhg-10l-min-50apm-50bpm-beauty-instrument-diaphragm-vacuum-pump [Last accessed: June 1, 2022].
- Honeywell. TruStability™ SSC Pressure Sensors. Honeywell; 2024. Available from: https://sps.honeywell.com/us/en/products/advanced-sensing-technologies/healthcare-sensing/board-mount-pressure-sensors/trustability-ssc-series [Last accessed: June 1, 2022].
- 37. Marchese AD, Katzschmann RK, Rus D. A recipe for soft fluidic elastomer robots. Soft Robot 2015;2(1):7–25.
- 38. Schmitt F, Piccin O, Barbé L, et al. Soft robots manufacturing: a review. Front Robotics Al. 2018;5. Publisher: Frontiers.

Cite this article as: Young TR, Yong YK, Fleming AJ (2025) Multivalve configuration for soft robotics: overcoming the trade-off between speed and accuracy in pneumatic systems. *Robotics Reports* 3:1, 54–64, DOI: 10.1177/28350111251380262.

Abbreviations used

2/2 valve = 2-way, 2-position valve 3/2 valve = 3-way, 2-position valve 3/3 valve = 3-way, 3-position valve 5/3 valve = 5-way, 3-position valve PneuSoRD = Pneumatic Soft Robot Drive rmse = root mean square error

rmse = root mean square error rms = root mean square

Publish in Robotics Reports



- Immediate, unrestricted online access
- Rigorous peer review
- Compliance with open access mandates
- Authors retain copyright
- Highly indexed
- Targeted email marketing

liebertpub.com/rorep